Engineering Pavement Design for Major Campus Road Network within Schist and Quartzite Dominated Rocks of Ondo State, Southwestern Nigeria

Abayomi Solomon Daramola [1], **Olumuyiwa Olusola Falowo*[2]**, **William Kunle Olabisi [3]**

[1]Rufus Giwa Polytechnic Owo, Department of Civil Engineering Technology, Ondo State Nigeria, oofalowo@futa.edu.ng
[2]Federal University of Technology Akure, Department of Applied Geology, Ondo State Nigeria, yomidams02@gmail.com
[3]Rufus Giwa Polytechnic Owo, Department of Civil Engineering Technology, Ondo State Nigeria, oolabisiwilliam@gmail.com

Abstract

The overall performance of new pavements depends on the quality of design based on comprehensive soil investigation. Due to recent expansion and opening up of remote places in the main campus of Rufus Giwa Polytechnic, Owo, Southwestern Nigeria, there's need to design and construct additional low volume roads to link up many newly constructed lecture theatres and administrative buildings, within schistose quartzite and quartzite rocks. The pavement thickness was derived using the AASHTO design method, after thorough traffic count, and estimated single axle load (ESAL) computation (19.97 msa) for 20 years projection. The soil properties in terms of CBR and subgrade modulus were determined using DCPT and empirical correlations. The quartzite environment showed slight competence over the schistose quartzite derived soils, with average penetrative index, CBR, effective modulus of subgrade of 0.7 mm/blow, 48 %, 15.64 ksi, and 0.88 mm/blow, 50 %, 15.57 ksi respectively. The flexible pavement design process generated thickness (wearing, base, and subbase courses) of 375 mm in schistose quartzite, and 366 mm in quartzite environment, for structural number (SN) of 3.18 and 3.16 respectively, while 243 mm was obtained for the rigid pavement. This thickness is sufficient in view of slight variation in the strength of the subgrade across the two geological formations in the area; traffic volume; and geology of the area. Consequently, these design thickness is adequate for area, based on rigidity, durability, longevity and ease of maintenance desired.

1. Introduction

Roads are crucial pieces of infrastructure for a nation's economic health; in fact, they quickly boost economic growth in emerging nations [1]. Given the importance of roads to a country's overall development and progress, they must be properly planned for and the right survey and study must be conducted to address issues like landslides, erosion, floods, and embankment subsidence [2]. The chosen alignment, specification, and design will therefore probably show flaws during execution if sufficient analysis is not

done. This will undoubtedly impact the project's budget, cause needless delays, and create contractual issues, all of which might lead to the project's collapse [3-4]. Rigid pavement made of cement concrete, is one that transmits loads to the subgrade with resilient bending resistance. One of the primary advantages of embracing concrete pavement are its strength, durability and ability to retain form [5-6]. It also spreads the stresses induced by wheel load, which are adequately reduced owing to its rigidity. Flexible pavement permits for significant deformation in subjection to high loads, which implies the road will deform/bend when strained [2, 7]. When stressed, stiff pavement maintains its form; nevertheless, it shatters, if the tension is high. Hence, the load is dispersed over a wider area. Rigid pavements have a strong flexural structure that allows wheel load stresses to be transferred to substantial area below. They can be constructed directly on subgrade or as only stratum of granular or stabilized material, as opposed to flexible pavement, which is laid on a prepared subgrade [3, 8].

Subgrades are crucial in flexible pavement design because they give the pavement structure structural stability when it is subjected to stress from traffic [9-10]. Under unfavorable loading and weather circumstances, traffic loads must be transmitted so that the subgrade distortion or deformation stays within elastic bounds and the shearing forces generated stay within safe limits. Unbound earth components like sand, silt, and clay make up the local sub-grade, which affects how roads are designed and built [4, 6]. Road design and performance depend heavily on the evaluation of soil subgrade characteristics, including density, stiffness, strength, and other in-situ metrics [11-12]. Traditionally, the CBR method or elastic deformations are taken into account while designing pavements. There are several design philosophies for flexible pavement, such as layered elastic and finite element techniques, which have a stronger foundation in the theory of material mechanics [13]. The CBR methodology is still one of the most dependable pavement design techniques, even with the advancements in these state-of-the-art approaches. This study adopted it in order to ensure that the proposed pavement has a suitable design life, before any rehabilitation is required. The time frame for which the originally planned pavement construction will last prior to any restoration is known as the design life or performance period [6].

This study aims to provide the asphaltic (flexible) and concrete (rigid) pavement thickness that would be sufficient for proposed pavement in Rufus Giwa Polytechnic Owo, (RUGIPO) Southwestern Nigeria, across schistose quartzite/quartz schist and quartzite rocks. The study is projected to determine the vehicular traffic load, by conducting a classified traffic count and analysis of the proposed pavements; and determination of the engineering characteristics of the foundation soil using dynamic cone penetration test (DCPT). RUGIPO is the only polytechnic educational institution in Ondo State, southwestern Nigeria, founded in 1979, with few structures and buildings. But with recent population trend, the institution is really expanding rapidly, hence a call for more additional roads.

2. Material and Method

2.1. The Study Area

Rufus Giwa Polytechnic in Owo, southwest Nigeria, is the research location (Figure 1). The institution is sited between the Universal Traverse Mercator (UTM) coordinates of Northing 798500 – 801500 m and Easting 781000 – 784000 m in the northeastern part of Ondo State. The annual rainfall in the region is above 1500 mm (on the average), and the temperature ranges between 24 and 28°C [14-15]. To identify various rock types, intricate rock associations, and certain structural components around the research area, geological field mapping was done across the institution's campus. The predominant rock types, which mostly trend roughly north-south, include gneisses, quartz-schist, granite, and quartzite (Figure 2). The granite and the gneisses are low lying and underlay the schistose quartzite/quartzite rocks in many places rocks. However, they also occur as ridges towards the eastern and central parts of the institution. The schistose-quartzite rock showed conspicuous schistocity. Observable tectonic imprints including foliation, faults, joints, and folds are also evident on the rocks.
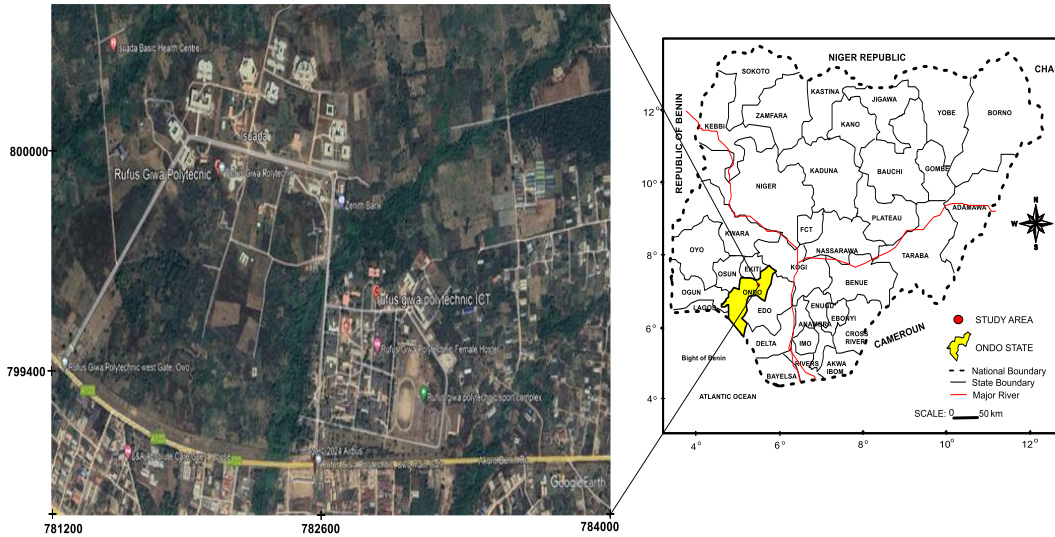
Figure 1. Research Location on (a) map of Ondo State and Nigeria (b) Google map

2.2. Preliminary/Reconnaissance Survey

This involves gathering and recording important information relating to the physical features of the proposed and existing roads in the institution. This involved important features such as topography, drainage system, nature of superficial soil layer, length of the proposed roads, geology or rock types, steams and vegetation [16]. After these information were gathered, the area were pegged for in-situ geotechnical investigation [17].

2.3. Geotechnical Investigation

However, digging test trenches at appropriate intervals along the road is the standard destructive testing technique. These are highly helpful since they allow for the measurement of pavement thicknesses and the removal of material for laboratory testing. However, test pits are seldom excavated at intervals of less than two to three kilometers and are costly to dig and restore [4, 9, 10, 11]. The in-situ geotechnical field method adopted was DCPT based on simplicity, cost, and speed [18-21].

The purpose of deploying this technique, was to obtain important geotechnical parameters such as CBR, subgrade strength coefficient, the DCP index, etc., which would be needed for the design of road [22-25], in relation to AASHTO method of flexible roadway design [26]. The analysis period for the proposed roadway is 20 years as shown in Table 1. The DCPT was carried out in thirty three selected points along proposed road environment even though the alignment has not been drawn or defined. The test was cut across the quartzite schist and quartzite rocks. Consequently, recordings were made separately on both geological formations to see how variation in the design parameters. In carrying out the test, the equipment was first placed above the natural soil over even surface. The test was carried out on the subgrade layer. Initial scale reading was noted and an eight kg hammer was dropped from a height of 575 mm [8, 27]. For every 100 mm scale reading, numbers of blows are recorded. The test was carried out till the penetration cone penetrates to a sufficient depth of subgrade [8, 28-29]. The readings were recorded in a standard format. The same procedure was repeated for all the test locations. The location map of the test points is shown below in Figure 3. The UK DCP 3.1 software was used for the analysis and interpretation of the data collected [8, 28-30]. The DCPT was done when the study site is at its maximum moisture content [31]. CBR was calculated using the Transport and Road Research Laboratory (TRL) relationship [32] in equation 1, and modified for moisture (water) content as shown in Table 2.

$$\text{Log}_{10}^{(CBR)} = 2.48 - 1.057 \, \text{Log}_{10}^{(\text{pen rate})} \tag{1}$$
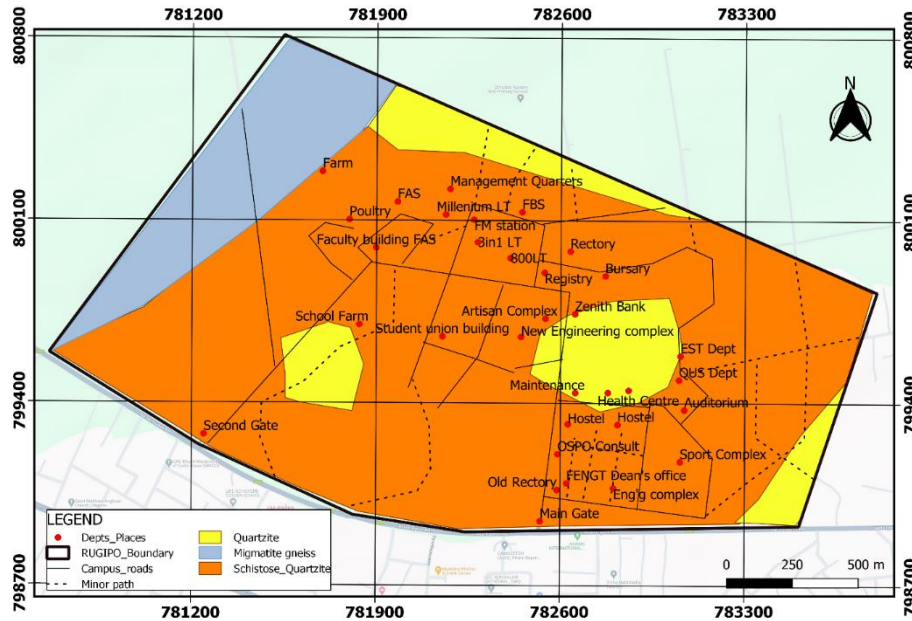
Figure 2. Geological map of the Campus showing predominant schistose quartzite formation (Source: Geological field mapping, 2022)

2.4. Design Parameters
2.4.1. Traffic Count and Estimate Single-axle load Computation

Classified volume counts (traffic survey) was done for two weeks (fourteen days) by taking record of all vehicles traversing the count point in each direction in the institution per day. The count points are denoted as TRC-1 and TRC-2, hence from the values obtained, the design thickness for pavement was estimated [3, 8]. The classified traffic volume counts at two locations were undertaken continuously for 10 hours. The survey was carried out between 7:00am to 5:00pm corresponding to peak or maximum period of traffic. The obtained data was converted to annual average daily traffic (AADT) and equivalent standard axle load (ESAL), which is summarized in Table 3. However, bicycle, tricycle, and motorcycle were neglected. The traffic count was based on the total number of equivalent standard axle loads (ESAL), the standard axle load being 80 kN. The ESAL is usually calculated from the axle load studies, and converting the actual axle loads to 80 kN axle loads, using equivalency factors, which depends on type of pavement, structural number, thickness of pavement, terminal pavement serviceability, and index, whether the axles are single, tandem or tridem [6]. The traffic data collected was projected at annual rate of 10 % to the year 2044 (20 years projection) based on Table 1 for low volume, paved road. The number of vehicles estimated for year 2044 was converted into cumulative ESAL.

Table 1. Analysis period according to AASHTO [26]

Pavement conditions	Analysis period years)
High volume, urban	30 – 50
High volume, rural	20 – 50
Low volume, paved	15 – 25
Low volume, aggregate surface	10 - 20

Table 2. CBR Adjustment Factor according to TRL [32]

Surface moisture	Ratio of in-situ moisture to OMC (modified AASHTO)	Default CBR Adjustment Factor
Wet	1	1
Moderate	0.75	0.71
Dry	0.5	0.51
Very dry	0.25	0.37
Unknown (not assessed or difficult to assess	-	0.5

2.4.2 Trend Analysis

For the purposes of economic analysis, pavement design, and geometric design, future traffic estimate is crucial [8]. Hence for this study, equation 2 was used in predicting the number traffic (calculated to be 2153) in the next 20 years.

$$T_n = T_0(1+r)^n \qquad\qquad (2)$$

Where n is number of years, T0 traffic in the year 0, T_n is traffic in year n, r is rate of growth. Consequently based on the annual average daily traffic, the standard axles (cumulative) was projected for 20-year design period, and was estimated to be 19.97 msa using equation 3.

$$N_s = \frac{365 \times A \times VDF[(1+r)^n - 1]}{r} \qquad\qquad (3)$$

where "N_s" is cumulative number of standard axle for the design, "A" is initial traffic of commercial vehicles per day, duly adjusted to account for traffic lane distribution according to Table 4 (0.80), "r" is yearly growth rate of commercial traffic, "n" is design lifespan in years, VDF is vehicle damage factor. The VDF (3.0) was obtained using Table 5.

2.4.3 Reliability of pavement design performance (R %)

This is a probabilistic approach, whereby each design factor is assigned an appropriate factor of safety, with a mean and variance. In other words, is the likelihood a pavement designed using the AASHTO [26] design empirical method will perform acceptably irrespective of traffic and environmental circumstances for its design lifespan [3, 8], as shown in Table 6. The reliability factor FR is estimated using equation 4:

$$log 10 FR = -Z_R S_o \qquad\qquad (4)$$

where FR is reliability factor obtained from Table 6, and is standard normal variant for given reliability (R %) obtained using Table 6. The standard deviation range was taken to be 90%. A standard deviation of 0.45 is appropriate for a flexible pavement and 0.35 for rigid pavements (Tables 7 - 8).

Figure 3. DCPT taken on site

Table 3. Annual Average Daily Traffic

S/N	Vehicle class	Average Axle weight (kg)	TRC-1	TRC-2	AVG	Equivalence factor	ESAL	ESAL vehicular distribution (%)
1	Small car	1100	107	93	100	0.0012	26.95	31.3
2	Medium car	1400	82	69	76	0.0016	26.068	23.6
3	SUV	2000	38	24	31	0.0022	15.19	9.7
4	Hilus	2000	24	18	21	0.0022	10.29	6.6
5	Vans	3500	18	22	20	0.2552	17.15	6.3
6	Ambulance	5000	5	8	7	0.1618	8.575	2.0
7	Taxi	5000	40	36	38	0.1618	51.44571	11.9
8	Small bus	6500	4	3	4	0.0246	7.039939	1.1
9	Medium bus	7500	4	8	6	0.0283	13.46597	1.9
10	Large bus	8500	3	7	5	0.0729	209.1407	1.6
11	Truck 2 axle	9000	2	1	2	0.1092	7.270861	0.5
13	Truck 3 axle	10000	1	2	2	0.1663	12.1181	0.5
14	Multi axle	12000	8	12	10	0.3281	2407.778	3.1
15	Total				320		2812.483	

Source: Fieldwork, 2024

Table 4. Lane Distribution Factor [6]

Number of lanes in each direction	Percentage of ESAL in design lane
1	100
2	80 – 100
3	60 – 80
4	50 - 75

Table 5. Values of VDF [6]

Number of commercial vehicle per day	Terrain	
	Rolling/Plain	Hilly
0 – 150	1.5	0.5
150 – 1500	3.5	1.5
More than 1500	4.5	2.5

Table 6. Reliability levels [26]

Highway class	Recommended reliability	
	Urban	Rural
Interstate and other freeways	85 – 99.9	80 – 99.9
Principal arterials	80 – 99	75 – 95
Collectors	80 – 95	75 – 95
Local	50 - 80	50 - 80

Table 7. Standard normal deviate for different values of reliability [26]

Reliability (%)	Standard normal deviate (Z_R)
50	0.000
60	-0.253
70	-0.524
85	-0.841
90	-1.282
95	-1.645
99	-2.327
99.9	-3.090

Table 8. Suggested Levels of Reliability for various Functional Classification [26]

Pavement	
Flexible	0.40 – 0.50
Rigid	0.30 – 0.40

2.4.4 Performance Criteria

The state of pavement can be assessed using present serviceability index (PSI), which has a range of 0-5. The 0 value denotes bad/impossible to travel pavement and 5 demotes perfect pavement. The difference between initial and final serviceability indexes (P_o and P_t) is called serviceability loss (ΔPSI). The ΔPSI is the main foundation for pavement design is. A value of 2.5 is commonly adopted for major (high traffic) highways, whereas 2.0 is tolerated for highways with lower traffic [6].

Using the above parameters, the thickness of the proposed flexible pavement followed AASHTO design equation, as shown in Equation 5.

$$logW_I8 = Z_r S_o + 9.36\log(SN + 1) - 0.20 + \frac{\log(\frac{\Delta PSI}{4.2 - 1.5})}{0.4 + \frac{1094}{(SN + 1)^{5.19}}}$$
$$+ 2.32\log M_r - 8.07 \qquad (5)$$

where; WI8 is Predicted number of 18-kip ESAL, Z_r is standard normal deviate, S_o is combined standard error of the traffic prediction and performance prediction, ΔPSI is difference between the initial design serviceability index P_0 and the design terminal serviceability index P_t, M_r is resilient modulus in psi, SN is structural number.

2.4.5 Determination of Resilient Modulus

One essential soil parameter that gauges soil stiffness is the effective roadbed modulus. It is employed in mechanistic pavement thickness design and is impacted by applied loads, soil physical characteristics, stress state, and soil type structure [24-25, 33]. Aside from CBR, resilient modulus (M_R) was also measured since the subgrade layer affects pavement performance. Either directly from the DCP data or indirectly from the relationship between subgrade modulus (M_R) and CBR, the subgrade resilient modulus may be ascertained. Hence for this study, it was derived using the relationship (equation 10) according to Carter and Bentley [34].

$$M_R(Kpa) = -3279PI + 114100 \qquad (6)$$

2.4.6 Estimation of Pavement Structural Number

Structural Number (SN) is a metric that shows how strong the pavement layers and the entire pavement structure are (35). By multiplying the layer material specific coefficient by the layer thickness, one may experimentally determine the contribution of a base/sub-base layer to a pavement's overall structural number (SN), as shown in equation 7.

$$SN = \sum a_i d_i m_i = a_i d_i + a_2 d_2 m_2 + a_3 d_3 m_3 \qquad (7)$$

where; a_i a_2, a_3 are layer coefficients for the wear, base, and subbase respectively (Table 9); $d_1, d_2, d_3,$ are layer thickness (inches) of the wear, base, and subbase respectively; $m_2, m_3,$ are drainage coefficients for base and sub-base courses (Table 10). The layer coefficient a_1 for asphalt concrete wear course is a function of resilient modulus, given in Table 9.

2.4.7 The effective modulus of subgrade reaction

The concrete effective modulus of subgrade reaction (K, in psi) increases with its strength. It determines the relative stiffness of the slab, and hence is a governing factor in design. The concrete elastic modulus (E_c) in psi is related to compressive strength ($f_c' = 3500\ psi$) as shown in equation 8. The typical compressive strength of concrete ranges from 2500 – 5000 psi. However, this range values can vary depending on the intended use. It can also be estimated from the characteristic cube strength of concrete. For this study, the compressive strength of the concrete was 3500 psi, and gives E_c of 3372165.48 psi.

$$E_c = 57000(f_c')^{0.5} \qquad (8)$$

Table 9. Surface Layer coefficient, with corresponding resilient modulus and CBR [26]

Resilient modulus (psi)	a_1	CBR	a_2	CBR	a_3
450,000	0.44	100	0.14	100	0.14
400,000	0.42	55	0.12	40	0.12
300,000	0.36	45	0.11	30	0.11
200,000	0.30	30	0.09	25	0.10
100,000	0.20	20	0.07	15	0.09
				10	0.08

Table 10. Modifiers, a_2 and m_3, for layer coefficients for drainage conditions [26]

Quality of drainage	Percentage of time pavement is exposed to moisture levels approaching saturation			
	Less than 1%	1 – 5%	5 – 25%	Greater than 25%
Excellent	1.40-1.35	1.35-1.30	1.30-1.20	1.20
Good	1.35-1.25	1.25-1.15	1.15-1.00	1.00
Fair	1.25-1.15	1.15-1.05	1.00-0.80	0.80
Poor	1.15-1.05	1.05-0.80	0.80-0.60	0.60
Very poor	1.05-0.95	0.95-0.75	0.75-0.40	0.40

2.4.8 Concrete modulus of rupture (S'_c)

The modulus of rupture (S'_c) or flexural strength for cement concrete, was incorporated into the design, by conducting cube test, and the value (average) after 28 days of curing was recorded. This value generally varies from about 39 to 56 kg/cm², however IRC suggests 38 – 42 kg/cm² for the initial design.

2.4.9 Load transfer coefficient

The capacity of a concrete pavement to transfer load over discontinuities, such joints or cracks, is taken into consideration by this coefficient, as shown in Table 11.

Table 11. Load transfer coefficient [26]

Shoulder	Asphalt		Tied cement concrete	
Load transfer devices	Yes	No	Yes	No
Plain jointed and jointed reinforced	3.2	3.8 – 4.4	2.5 – 3.1	3.6 – 4.2
CRCP	2.9 – 3.2	N/A	2.3 – 2.9	N/A

2.4.10 Drainage coefficient (Cd)

The drainage coefficient is dependent on the drainage's quality as well as the year-round moisture content and level. Excellent to extremely bad is the range of drainage quality classifications. For this study 0.90 was adopted from Table 12.

Table 12. Recommended values of drainage coefficient [26]

Quality of drainage	Percent of Time Pavement Structure is Exposed to Moisture Levels Approaching Saturation			
	Less than 1%	1 - 5%	5 - 25%	Greater than 25%
Excellent	1.25 – 1.20	1.20 – 1.15	1.15 – 1.10	1.10
Good	1.20 – 1.15	1.15 – 1.10	1.10 – 1.00	1.00
Fair	1.15 – 1.10	1.10 – 1.00	1.00 – 0.90	0.90
Poor	1.10 – 1.00	1.00 – 0.90	0.90 – 0.80	0.80
Very Poor	1.00 – 0.90	0.90 – 0.80	0.80 – 0.70	0.70

3   Results and discussion

3.1 DCPT Analysis

The result of the DCPT is presented in Table 13. The penetrative index ranged between 0.1 – 6.4 mm/blow, with an average of 0.83 mm/blow. Schistose quartzite recorded values ranging from 0.1 – 6.4, with an average of 0.88 mm/blow, while that of quartzite is between 0.1 and 1.9 mm/blow. This shows that quartzite offers more resistance to penetration than the schistose quartzite. This could as result of high micaceous minerals present in schistose quartzite (4). The range of cumulative number of blows recorded at average refusal depths of 619 mm (schistose quartzite) and 543 mm, are 56 – 123 (avg. 94) and 54 – 132 (avg. 100) respectively. The obtained CBR was a little bit higher in schistose environment (49.9 %) than quartzite derived soil (47.7 %). Based on analysis of the DCPT data, two layers were delineated within the penetrative depth (approximately 100 cm), and typical curves are shown in Figure 4. From the curves, the competent layer suited for the pavement design and construction ranged from 234 – 874 mm (avg. 587 mm) in schistose quartzite and 321 – 857 mm (avg. 501 mm) in quartzite derived soil, while the regional average is 565 mm. This implies that the upper 0.6 m of the soil must be excavated, so that the pavement can sit on competent subgrade soil.

The subgrade modulus reaction, which was determined from the DCPT penetrative index showed a regional average of 15.59 ksi, but slightly higher values were in quartzite (15.65 ksi), while the minimum value recorded fall within the schistose quartzite. Consequently, the quartzite derived soil showed more competence than schistose quartzite derived soils in the environment, even though the variance is very slight, however this cannot be overlook during the design stage, especially the flexible pavement design.

3.2 Traffic volume survey

The result of the classified traffic volume survey that was is presented in Table 3, the distribution showed that the small car (31.3 %), medium car (23.6 %), and taxi (11.9 %) had the highest percentage of road traffic (Table 3). The traffic count data was converted to AADT and ESAL, gives design load of 19.97 msa for the 20 years projection (design life).

3.3 Pavement Thickness

The pavement thickness derived from the design charts (36) as shown in Figures 5 and 6. The overall thickness of the rigid pavement is calculated to be 243 mm (9.6 inches). In case of flexible pavement, according to the DCP in-situ test analysis, the roadway is projected to embrace three structural layers (wearing course, base, and subbase) with the subgrade/foundation soil. The result of the flexible pavement thickness (for wearing course, base, and subbase) is 375 mm (14.8 inches) in schistose quartzite, and 366 mm (14.4 inches) in quartzite environment, for structural number (SN) of 3.18 and 3.16 respectively. These design thicknesses are adequate for 20 years of projection. The analysis of the each layer in both schistose quartzite and quartzite environment is shown in Table 14. The mean values inputted into equation 5, are presented in Table 15, while 241.3 mm (9.5 inches) was obtained on the design chart (Figure 6). Consequently, the design thickness derived from the DCP computation for the proposed flexible pavement is shown in Table 16, with the thickness of the subgrade taken to be 300 mm (11.8 in). This thickness is tolerable and sufficient for the pavement considering the traffic volume and geology of the area.

Table 13. Summary of the geotechnical Properties of the Investigated Soil

Sample No	East	North	Geology	PI (mm/blow) At Refusal	No. of blows	Depth at refusal (mm)	CBR (%)	Thickness (mm)	Depth (mm)	M_R (Ksi)
S1	783243	798963	Schistose quartzite	1.80	85	471	50	338	338	15.15
S2	783218	799254	Schistose quartzite	6.40	123	726	50	69	471	13.04
S3	782845	799543	Quartzite	0.10	96	794	50	69	471	15.93
S4	782706	799918	Schistose quartzite	0.10	96	794	50	63	794	15.93
S5	782659	800097	Schistose quartzite	0.30	108	473	50	222	473	15.84
S6	782963	798952	Schistose quartzite	0.70	93	668	92	177	668	15.65
S7	782575	798973	Schistose quartzite	0.30	117	387	50	194	387	15.84
S8	782593	799356	Quartzite	0.20	132	411	50	194	387	15.88
S9	783000	799192	Schistose quartzite	0.50	107	694	50	24	694	15.74
S10	782994	799342	Schistose quartzite	0.60	102	759	50	136	759	15.70
S11	783081	799481	Quartzite	0.40	94	748	50	166	748	15.79
S12	783164	799560	Schistose quartzite	0.40	95	746	50	282	371	15.79
S13	782555	799723	Quartzite	0.80	54	857	29	260	857	15.61
S14	782538	800002	Schistose quartzite	0.50	91	790	48	305	790	15.74
S15	782467	800242	Schistose quartzite	1.30	93	874	47	394	874	15.38
S16	782355	800179	Schistose quartzite	0.40	80	588	50	131	588	15.79
S17	782376	800269	Schistose quartzite	1.0	71	666	47	268	666	15.51
S18	782323	800650	Quartzite	0.80	75	610	50	212	610	15.61
S19	782179	800212	Schistose quartzite	0.20	79	479	50	127	479	15.88
S20	782169	799866	Schistose quartzite	0.20	110	595	50	188	595	15.88
S21	782091	799647	Schistose quartzite	0.40	101	697	50	220	697	15.79
S22	781975	799360	Schistose quartzite	0.40	97	438	50	139	438	15.79
S23	782353	799831	Schistose quartzite	1.60	94	841	34	553	841	15.24
S24	788275	799577	Schistose quartzite	0.40	108	690	50	223	690	15.79
S25	782259	799488	Schistose quartzite	0.20	88	366	50	127	366	15.88
S26	781869	800145	Schistose quartzite	0.20	63	234	50	118	234	15.88
S27	781818	800170	Schistose quartzite	0.80	56	408	49	226	408	15.61
S28	781797	800015	Schistose quartzite	1.70	107	853	31	744	853	15.19
S29	781680	800070	Schistose quartzite	0.60	94	624	50	183	624	15.70
S30	781563	799497	Quartzite	1.90	117	358	50	239	358	15.10
S31	781497	799617	Quartzite	0.50	97	321	50	176	321	15.74
S32	781474	799859	Quartzite	1.20	125	335	50	250	351	15.42
S33	781260	799322	Quartzite	0.50	114	450	50	158	450	15.74
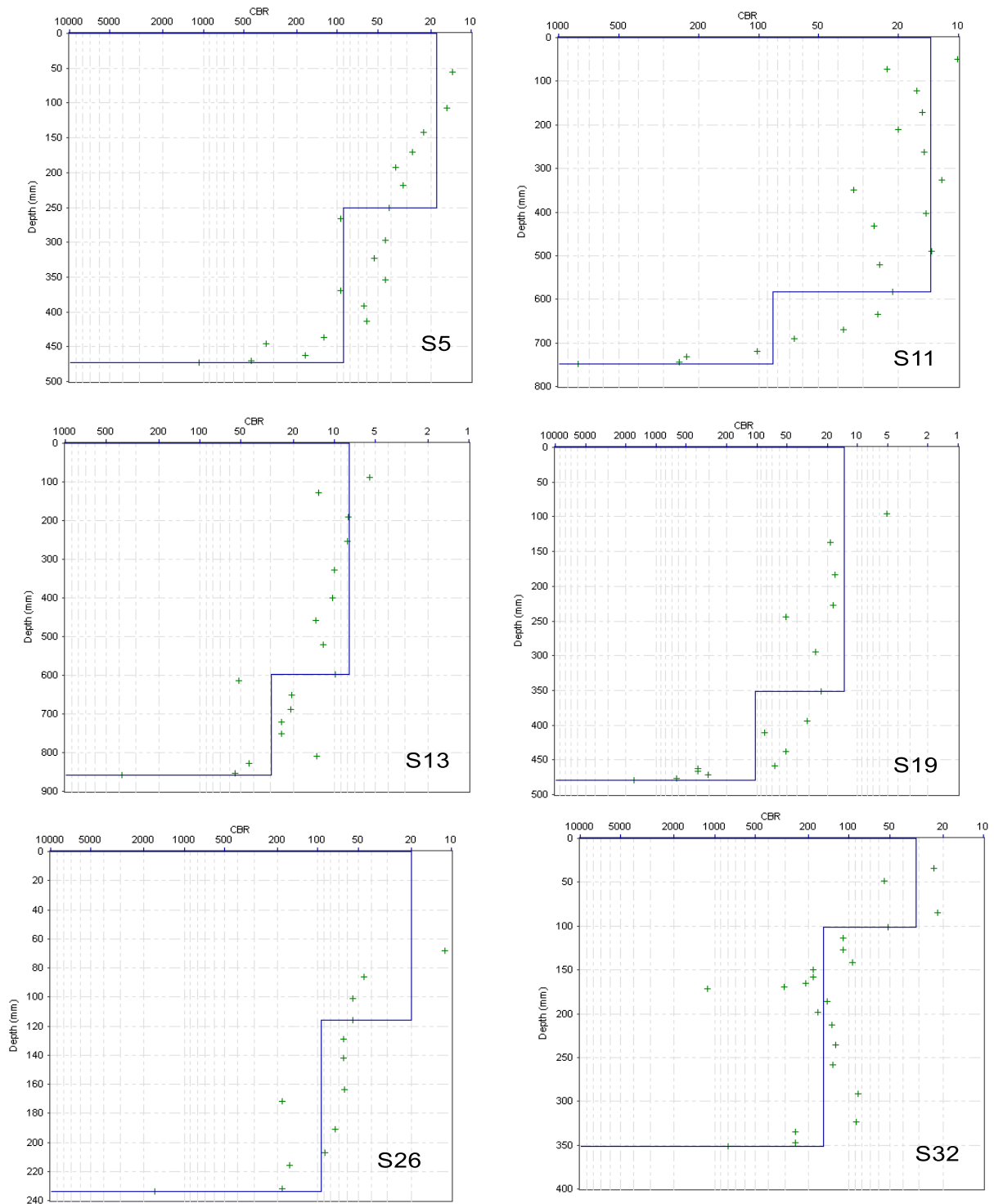
Figure 4. Typical curve obtained from DCPT, showing the plot of CBR (%) with depth/layer's thickness (mm) at different location points.
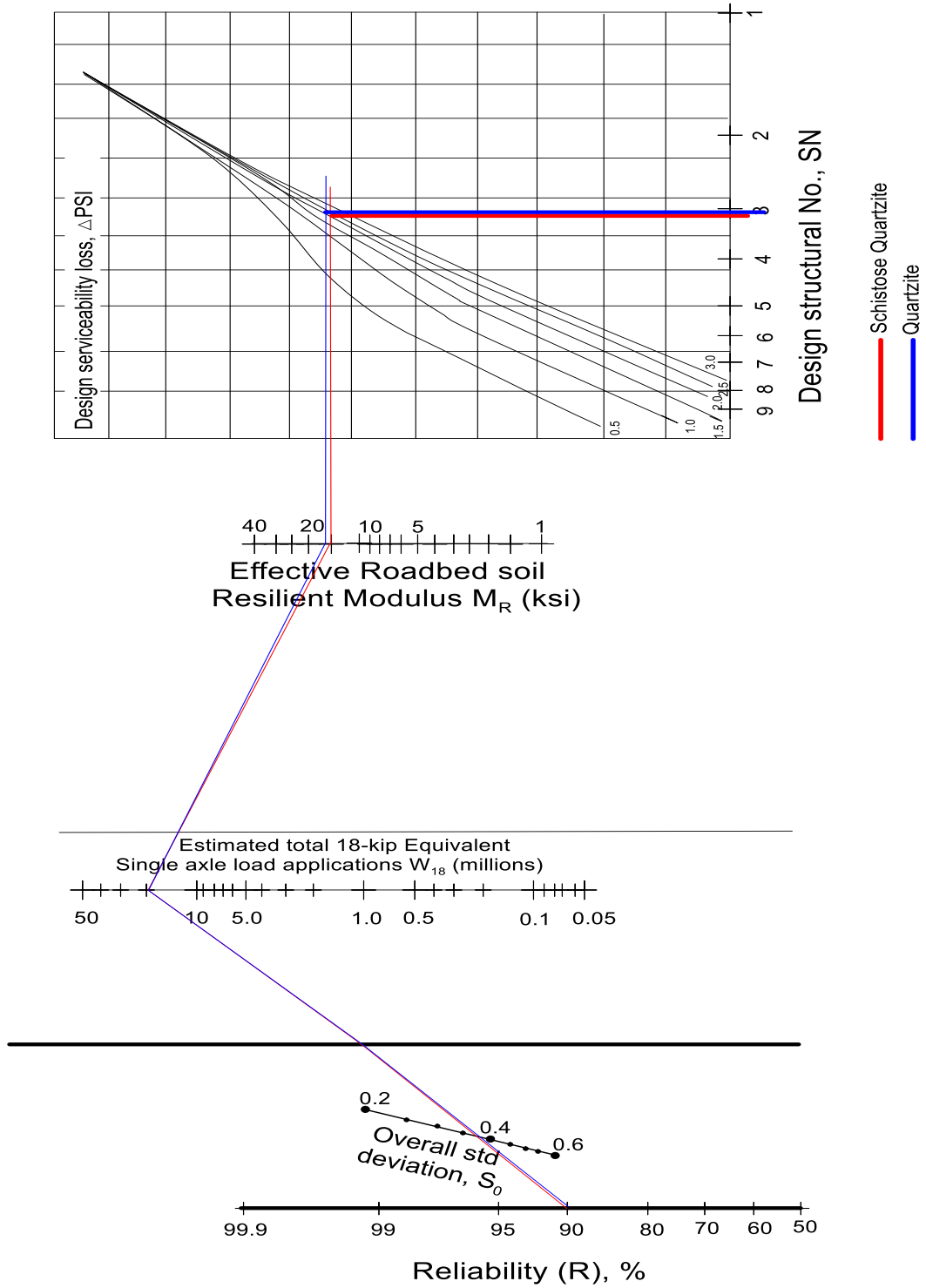
Figure 5. Design chart for flexible pavement based on using mean values, showing schistose quartzite and quartzite plots with close Structural Number
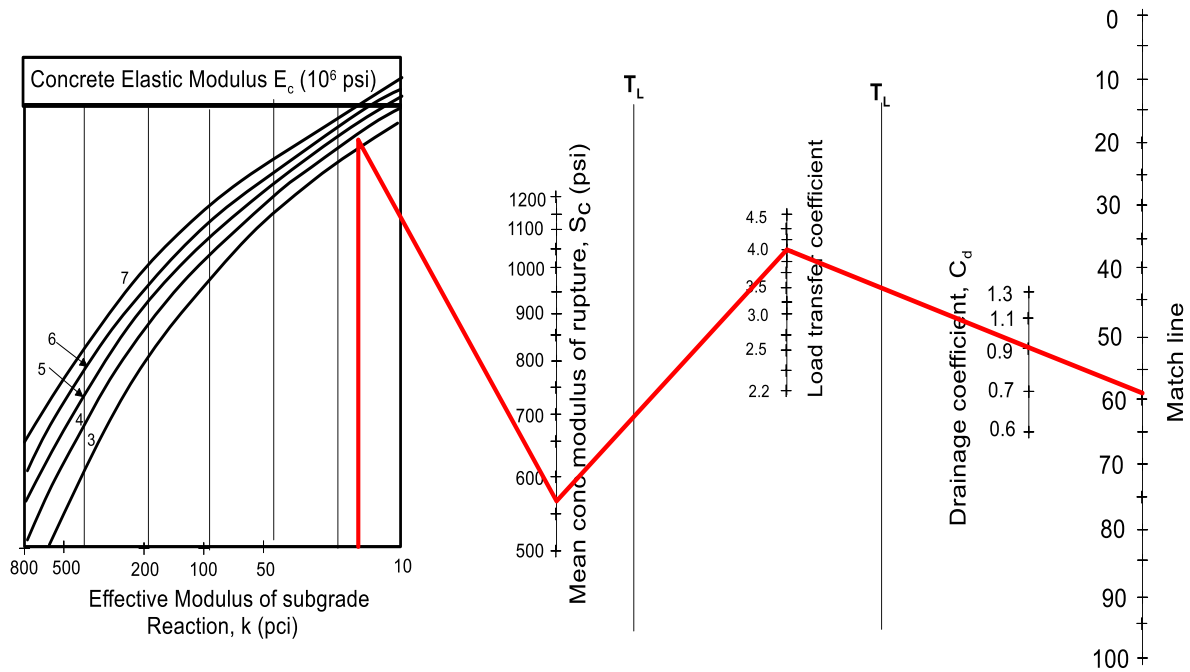
Figure 6a. Design chart for rigid pavement design showing the plot of the proposed design

Table 14. Flexible Pavement Layer details

Layer thickness	Quartzite	Schistose quartzite
Surface	50 mm	50 mm
Base	315 mm	320 mm
Subbase	301 mm	305 mm

Table 15. Pavement Evaluation Parameters

Parameter	Value
Subgrade CBR	49 %
Minimum thickness of subgrade	400 mm
Design Approach	AASHTO method
Concrete elastic modulus (10^6 psi)	3.4
Modulus of subgrade	15.59 ksi
Concrete modulus of rupture	569 psi
Load transfer coefficient	4.0
Drainage coefficient	0.9
Initial serviceability	4.0
Terminal serviceability	2.0
Serviceability loss	2.0
Overall Standard deviation	0.35
Reliability	0.90
Resilient modulus of subgrade	15.59 pci

Table 16. DCP Test Results obtained for the flexible pavement

Layer	Thickness (mm)	
	Quartzite	Schistose Quartzite
Wearing Course	50	50
Base	146	151
Subbase	170	174
Subgrade	300	300
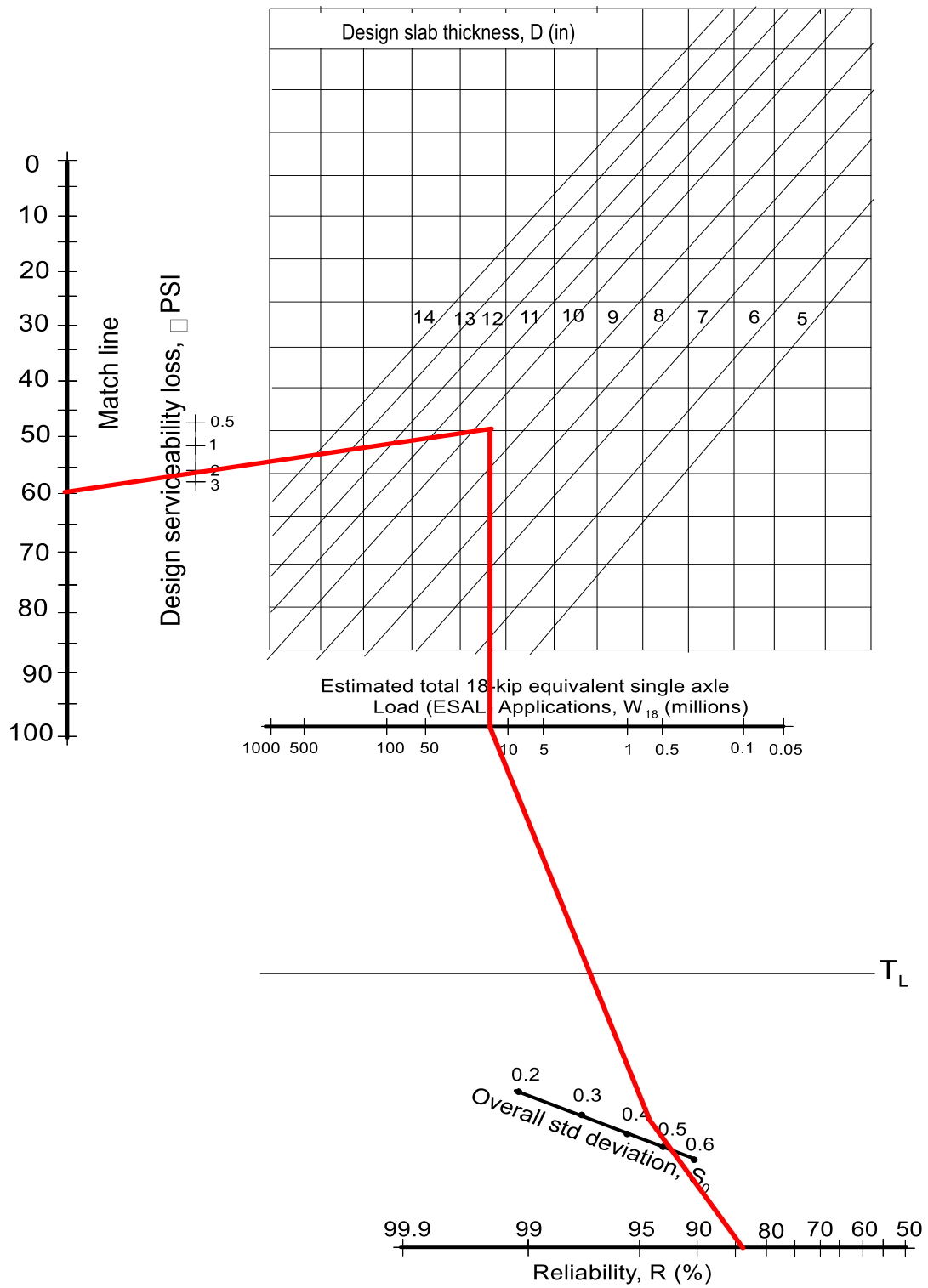
Figure 6b. Design chart for rigid pavement design (continued from Figure 44a)

4.   Conclusion

The design of flexible and rigid pavements for major campus road straddling schistose quartzite and quartzite dominated rocks in RUGIPO, Ondo State, Southwestern Nigeria has been completed. The DCPT data showed that the quartzite derived soil are slightly competent than schistose quartzite, with both having overlapping strength values in many locations. The flexible pavement design thickness (without subgrade) and structural number are 375 mm (14.8 inches) in schistose quartzite, and 366 mm (14.4 inches) in quartzite environment, for structural number (SN) of 3.18 and 3.16 respectively, for 20 years projection. The rigid pavement design gave a thickness of 243 mm (9.6 inches). This thickness is tolerable and adequate for the proposed pavement considering the 20 years projection, traffic volume and geology of the area. Therefore both design thickness and other parameters of the proposed pavements are therefore recommended. Nevertheless, the initial cost of constructing rigid road is very higher than flexible pavement i.e., usually doubled the cost of flexible road in Nigeria. Even though in the long run, the cost of maintaining flexible pavement can make the overall sum more costly than rigid pavement. Apart from this factor, the schistose quartzite/quartz schist is the most widespread rock in the area, whose major soil derivatives are sandy clay or clayey sand depending on degree of weathering. Thus, in most cases, the clayey/silty composition are usually higher in proportion to sand in many soil samples. Therefore, clayey soil (A-7-5/A-7-6) is usually susceptible to expansion as a result of wetting and drying, which the weather condition in the study will continuously enhance, since rainfall intensity is more than 1500 mm annually in the study area. Therefore, in light of these, the rigid pavement is recommended based on strength, maintenance cost, long term performance (20 years projection), durability, longevity/serviceability life-span, adaptability to extreme weather condition, lower water penetration potential, and less noise pollution (due to high degree of serenity expected in academic environment).

Author contributions:

Abayomi Solomon Daramola: Conceptualization, Investigation, Methodology, Software **Olumuyiwa Olusola Falowo:** Conceptualization, Investigation, Methodology, Data curation, Writing-Original draft preparation, Software, Validation. **William Kunle Olabisi:** Visualization, Investigation, Supervision, Writing-Reviewing and Editing.

Conflicts of interest

The authors declare no conflicts of interest.

References

1. Falowo, O. (2023). Application of Geoinformatics in Civil Engineering Design and Construction: A Case Study of Ile Oluji, Southwestern Nigeria. *International Journal of Environment and Geoinformatics (IJEGEO)*, 10(4): 117-145. doi. 10.30897/ijegeo.1262020
2. Zulufqar, B. R., Rakesh, G. (2017). Study of Defects in Flexible Pavement and its Maintenance.
3. Akintayo, F. O., Osasona, T. D. (2022). Design of Rigid Pavement for Oke- Omi Road, Ibadan, Oyo State. *FUOYE Journal of Engineering and Technology (FUOYEJET),* 7(3), 382-388. http://doi.org/10.46792/fuoyejet.v7i3.837
4. Bell, F. G. (2004). Engineering Geology and Construction. *Spon Press*, London, 2004.
5. Huang, Y. H. (2004). Pavement Analysis and Design, Prentice-Hall, Englewood Cliffs, NJ.
6. Kadyali, L. R., & Lal, N. B. (2008). Principles and Practices of Highway Engineering (Including Expressways and Airport Engineering) Fifth Edition, *Romesh Chander Khanna*, New Delhi, India, 858pp.

7. Milind, V., & Kadam, K. A. (2016). Comparative Study on Rigid and Flexible Pavement. *IOSR Journal of Mechanical and Civil Engineering*, Vol 13.
8. Quansah, A., Ntaryamira, T., & Obeng, D. A. (2017). Evaluation of Pavement Structural Life Using Dynamic Cone Penetrometer. *Int J Pavement Eng,* vol. XXX, no. XX, 1–7.
9. Wright, P. H. (1986). Highway Engineering, Sixth Edition, John Willey and Sons, New York, 1986.
10. Vazirani, V. N., & Chandola, S. P. (2009). Concise Handbook of Civil Engineering Revised Edition, Rajendra Ravindra Printers Pvt Ltd, New Delhi, India, 1318pp
11. Vandre, B., Budge, A., & Nussbaum, S. (1998). DCP- A Useful Tool for Characterizing Engineering Properties of Soils at Shallow Depths. *Proceedings of 34th Symposium on Engineering Geology and Geotechnical Engineering*, Utah State University, Logan, UT.
12. Paige-Green, P., & Van Zyl, G. D. (2019). A Review of the DCP-DN Pavement Design Method for Low Volume Sealed Roads: *Development and Applications. Journal of Transportation Technologies*, 2019 (9), 397-422.
    https://doi.org/10.4236/jtts.2019.94025
13. Hadi, M. N. S., & Arfiadi, Z. (2001). Optimum Rigid Pavement Design by Genetic Algorithms, *Computers and Structures.* Vol.1, No.5.
14. Iloeje, P. N. (1981). A new geography of Nigeria. Longman Nigeria Limited, Lagos.
15. Federal Meteorological Survey. (1982). Atlas of the Federal Republic of Nigeria, 2nd Edition, Federal Surveys, 160pp.
16. Falowo, O. O., & Dahunsi, S. D. (2020). Geoengineering Assessment of Subgrade Highway Structural Material along Ijebu Owo – Ipele Pavement Southwestern Nigeria. *International Advanced Research Journal in Science, Engineering and Technology (IARJSET)*, Vol 7, Issue 4, 10pp. DOI 1017148/IARJSET20207401
17. Falowo, O. O., Olorunda, O., Ologan, T., & Ayetoro, A. (2023). Baseline Geo-Engineering Dataset and Parameters' Empirical Modeling for Civil Engineering Construction in Okeigbo, Southwestern Nigeria. *International Journal of Earth Sciences Knowledge and Applications*, 5 (2): 182-207. http://www.ijeska.com/index.php/ijeska
18. Vakili, A. H., Salimi, M., & Shamsi, M. (2021). Application of the dynamic cone penetrometer test for determining the geotechnical characteristics of marl soils treated by lime. *Heliyon,* 7(9):e08062. https://doi.org/10.1016/j.heliyon.2021.e08062
19. Mejias-Santiago, M., Garcia, L., & Edwards, L. (2015). Assessment of material strength using dynamic cone penetrometer test for pavement applications. *Airfield Highway pavement*: 837-848.
20. Lockwood, D., de Franca, V. M. P., Ringwood, B., & de Beer, M. (1992). Analysis and classification of DCP survey data Technology and information management programme Pretoria, South Africa: CSIR Transportek.
21. Lee, J. S., & Byun, Y. H. (2020). Instrumented cone penetrometer for dense layer characterization. *Sensors*, 20(20): 5782. https//doi.org/10.3390/s20205782.
22. Livneh, M. (1989). Validation of correlations between a number of penetration tests and in situ California bearing ratio tests. *Transp Res Rec* 1219: 56-67.
23. Kim, S. Y., Lee, J. S., & Hong, W. T. (2021). Subgrade assessment using automated dynamic cone penetrometer to manage geo-infrastructures. *Smart Struct Syst.,* 27(5): 861-870.
    https://doi.org/10.12989/sss.2021.27.5.861
24. George, V., & Kumar, A. (2018). Studies on modulus of resilience using cyclic triaxial test and correlations to PFWD, DCP, and CBR. *Int J Pavement Eng*, 19(11): 976-985. https://doi.org/10.1080/10298436.2016.1230428
25. George, K. P., & Uddin, W. (2000). Subgrade characterization for highway pavement design, final report Jackson, MS: *Mississippi Department of Transportation*.
26. AASHTO (1993). Guide for Design of Pavement Structures. *American Association of State Highway and Transportation Officials*, Washington, DC.
27. Garber, N. J., & Hoel, L. A. (2009). Traffic and Highway Engineering, 3rd edition, Pacific Grove, CA: Brooks-Cole.
28. De Beer, M. (1990). Use of Dynamic Cone Penetrometer in the design of road structures, *Geo-techniques in African Environment*, pp. 167-176 (Balkema: Rotterdam).
29. Done, S., & Samuel, P. (2006). Department for International Development (DFID) Measuring road pavement strength and designing low volume sealed roads using the dynamic cone penetrometer Unpublished Project Report, UPR/IE/76/06 Project Record No R7783. www.transport-linksorg/ukdcp/docs/Manual/manualhtml
30. Alshkane, Y. M., Rashed, K. A., & Daoud, H. S. (2020). Unconfined compressive strength (UCS) and compressibility indices predictions from dynamic cone penetrometer index (DCP) for cohesive soil

Kurdistan Region/Iraq. Geotech Geol Eng, 38(4): 3683-3695. https://doi.org/10.1007/s10706-020-01245-1

31. Ashlesha, D., Kalinga, A., & Dhapekar, R. (2017). Study of rigid pavements – review. *International Journal of Civil Engineering and Technology (IJCIET)* Volume 8, Issue 6, pp. 147–152.

32. Transport and Road Research Laboratory (1990). A user's manual for a program to analyse dynamic cone penetrometer data (Overseas Road Note 8) Crowthorne: Transport Research Laboratory.

33. Falowo, O. O. (2023b). Geoengineering soil characterization and modeling of highway route along Owo–Ikare (F-215) pavement, Southwestern Nigeria: towards reconstruction/rehabilitation. Arabian Journal of Geosciences (Springer Publication), 16:499, pp. 25. https://doi.org/10.1007/s12517-023-11606-8

34. Carter, M., & Bentley, S. P. (1991). Correlations of soil properties, *Pentech Press Publishers*, London, 129pp

35. Nam, B. H., An, J., Kim, M., Murphy, M. R., & Zhang, Z. (2018). Improvements to the structural condition index (SCI) for pavement structural evaluation at network level. *International Journal of Pavement Engineering*, 17(8):680–697.

36. Maharaj, D. K., & Gill, S. (2014). Development of Design Chart for Rigid Pavement by Finite, Element Method. *International Journal of Latest Research in Engineering and Computing*, Vol.2: Issue 2, March-April, pp.27-39.